High quality thermochromic VO2 thin films deposited at room temperature by balanced and unbalanced HiPIMS

Jean-Louis Victor, Corinne Marcel, Laurent Sauques, Nicolas Penin, Aline Rougier

High quality thermochromic VO_2 thin films deposited at room temperature by balanced and unbalanced HiPIMS

J.L. Victor[a,c], C. Marcel[a], L. Sauques[b], N. Penin[c], A. Rougier[c*]

[a] CEA-DAM, Le Ripault, Monts F-37260, France
[b] Centre d'Expertise Parisien de la Délégation Générale à l'Armement, Paris F-75015, France
[c] CNRS, Univ. Bordeaux, Bordeaux INP, ICMCB (UMR 5026), Pessac F-33600, France
* corresponding author : aline.rougier@icmcb.cnrs.fr

Abstract

In this paper, vanadium dioxide thin films were successfully deposited at room temperature by high power impulse magnetron sputtering (HiPIMS) using two different magnetron configuration: *(i)* a conventional balanced magnetron and *(ii)* an unbalanced magnetron. In the case of the unbalanced magnetron, the magnetic field is extended towards the substrate and the energetic ions in the plasma actively participate in film growth allowing to improve film crystallinity. The as-deposited thin films were annealed under Ar flow for 1 h to obtain thermochromic VO_2(M) phase. The 120 nm films were first characterized at room temperature by X-ray diffraction (XRD). Then, the thermochromic behavior of the VO_2 films was investigated by electrical and optical characterizations. The effect of annealing temperature on thermochromic properties of VO_2 was studied showing that high quality VO_2(M) film can be obtained at 300 °C using unbalanced HiPIMS. A very efficient change in transmittance exceeding 70 % is observed in the IR spectral region. This investigation demonstrates the capability of using unbalanced HiPIMS to achieve high optical performances for VO_2 at lower temperature as well as the potential of this technology for the deposition of VO_2(M) films onto temperature-sensitive substrates.

Keywords

Vanadium dioxide, high-power impulse magnetron sputtering, balanced and unbalanced magnetron, thermochromic thin films, low annealing temperature, IR characterization.

1. Introduction

Chromogenic materials allow the modulation of the solar energy under the action of an external stimulus and can be used for a wide range of technologies [1, 2, 3]. Among them, thermochromics are materials in which observable changes of optical properties are induced by a change of temperature.

Vanadium dioxide (VO_2) is a thermochromic oxide showing a first order and reversible phase transition at the critical temperature Tc ≈ 68 °C [4]. It transits from a low-temperature semi-conductive phase (monoclinic structure, *P21/c*) to a high temperature metallic phase (rutile-type structure, *P42/mnm*). The phase transition is accompanied with drastic changes in physical properties (optics, electronics and magnetic). As the optical variation across the transition occurs at infrared wavelength, VO_2 has become a promising candidate for many applications requiring thermal fluxes regulation upon temperature such as smart radiator devices [5], adaptive thermal camouflage [6] or smart windows [7].

Several chemical and physical methods have been developed to grow dense and continuous VO_2 based films including chemical vapor deposition (CVD), sol-gel, pulsed laser deposition (PLD), magnetron sputtering, etc. [8, 9, 10, 11]. Among them, the films prepared by reactive magnetron sputtering exhibit excellent properties (high density and good uniformity) and easy industrialization. Unfortunately, in the case of standard magnetron sputtering such as direct current magnetron sputtering (DCMS) or radio frequency magnetron sputtering (RFMS), the fabrication of VO_2 requires high annealing temperatures, i.e. above 400 °C for material crystallization [12]. Consequently, the elaboration of VO_2 in thin films is not compatible with

temperature-sensitive substrates. High power impulse magnetron sputtering (HiPIMS) is a novel sputtering method, applied recently to the deposition of VO_2 films [13, 14, 15]. It is characterized by a high target current and thus a production of highly energetic sputtered ions [16]. The energy of the deposition flux can be controlled via substrate bias voltage and the large flux of sputtered species provides additional energy increasing the surface diffusion and hence increasing the nucleation density. The preparation of highly crystallized VO_2 films at lower temperature can thus be achieved. Fortier et al. [17] and Aijaz et al. [18] reported thermochromic crystalline VO_2 thin films by HiPIMS at a temperature deposition of 300 °C using a substrate bias voltage. More recently, Houska et al. [19] achieved VO_2 films by HiPIMS on amorphous glass substrates using the same "low" temperature of 300 °C without any bias voltage.

Magnetic field design of the magnetron is also an important parameter in HiPIMS affecting the plasma and the film deposition. The magnetron device consists of dipole configuration to trap the electrons emitted at the cathode in the sputtering system. The magnetic field configurations with different field strengths may alter the plasma distribution from the target to the substrate. Two configurations can be used for thin films deposition; conventional balanced magnetron (BM) and unbalanced magnetron (UBM) (*Fig. 1)*. In the case of a conventional balanced magnetron, the magnetic field is localized near the target. Under UBM the magnetic field extends towards the substrate and the energetic ions in the plasma gain high energy and actively participate in film growth through enhanced migration of adatoms. It has been observed that UBM improves the film density and crystalline quality of the deposited thin films [20]. Such a magnetron configuration could be used for deposition of high quality thermochromic VO_2 films at lower temperature. However, as far as we know, no literature has yet been reported on this topic.

In this work, VO_2 thermochromic thin films were deposited on glass and silicon substrates at room temperature by both balanced and unbalanced HiPIMS. Neither substrate bias nor crystalline interlayer were used. Thus, the deposition process reported in this paper can be classified as industry-friendly. An annealing treatment was performed in a furnace outside of the deposition chamber to crystallize VO_2 films and the effect of the operating temperature on the thermochromics properties was studied. Several temperature dependence characterizations such as optical transmittance in the mid-infrared range, resistivity and infrared thermography were performed to investigate the thermochromic behavior of the films. The main aim of this work is to demonstrate the benefits of using unbalanced HiPIMS to obtain functional VO_2 thin films at lower temperature.

2. Experimental section

2.1. VO_2 thin films deposition

VO_2 thin films were grown at room temperature using a turbomolecular pumped magnetron sputtering system (ALLIANCE CONCEPT) equipped with a HiPIMS power supply. Two magnetron configurations were used: *(i)* a conventional balanced magnetron (BM) produced by BALZERS and *(ii)* an unbalanced magnetron (UBM) produced by DEPHIS. Silicon and glass substrates (2.5×2.5 cm^2) were placed at a distance of 10 cm from a high purity vanadium target (75×22.5 cm^2) (99.9 % GENCOA). The Si-(001) substrate was selected for its optical transparency in the infrared range. The substrates were not heated during the whole deposition process.

As sputtering and reactive gas, high purity Ar and O_2 were introduced into the chamber by using two mass flow controllers. During the deposition process, for a total sputtering pressure of 0.7 Pa, Ar and O_2 gas flow rates were fixed at 100 sccm and 12.85 sccm, respectively. The HiPIMS power was supplied with a pulse frequency of 1 kHz and a pulse on-time of 30 μs

that resulted in a duty cycle of 3%. An average current of 6 A was used during all experiments.

Fig. 2 shows the time-dependent waveforms of the current and the voltage during the HiPIMS discharge employed for VO_2 films elaboration. The peak current density reaches 0.3 $A.cm^{-2}$ during the discharge, which is about two orders-of-magnitude higher than that obtained under conventional DCMS conditions. Such a current allows to increase the ionized deposition fluxes, resulting in a better crystallinity and density of the films. Before each deposition, vanadium target was pre-cleaned in pure argon for 5 min to remove metal oxide impurities. Discharge parameters were systematically checked during the process to be sure the optimized regime had been reached. Deposition rate was very stable and reproducible, with a mean value 25 ± 0.5 nm/min. So, the film thickness could be directly related to the sputtering time.

2.2. Annealing treatment

In order to crystallize the as-deposited VO_2 films, an annealing treatment was performed under Ar flow for 2 hours. Both heating and cooling rates were adjusted at 2 $°C.min^{-1}$ and the Ar gas flow was fixed at 0.5 $L.min^{-1}$ during the whole process. Three different annealing temperatures were tested: 300 °C, 400 °C and 500 °C.

2.3. VO_2 thin films characterization

The thickness of the films was measured with a Veeko Dektak 8 profilometer. The structure of the films was identified by Bruker D8 Discover X-ray diffraction at a grazing angle of 2° using CuKα radiation source (λ = 1.54056 Å) in a 2θ range from 10° to 50°. The composition was examined by Rutherford backscattering spectrometry with 2 MeV He ions at

a scattering angle of 170°. Rutherford simulation program (SIMNRA) was used to simulate the RBS spectra.

The films resistivity was measured with a standard four-point system. Four small probes in contact with the sample were linearly aligned with equal spacing between them. Current was sent from ADRET 103A generator through the outer probe, while the voltage difference between the inner probes was measured by a voltmeter. The film resistivity was then obtained from current-voltage characteristic. The spectral transmittance in the wavelength range of 2.0 µm – 25 µm at normal incidence was measured using Fourier transform infrared spectroscopy (FTIR, Bruker Vertex 70v). Both resistivity and transmittance measurements were carried out between 20 and 100 °C, while a thermocouple was positioned very close to the films.

The LWIR thermal images of VO_2 thin films deposited on glass substrate were taken at different temperatures using IR camera in the 7.5–13 µm region (FLIR system). Heating and Peltier cooling elements allowed to control the sample temperature precisely.

3. Results and discussion

3.1. Study of VO_2 thin films prepared by balanced HiPIMS and annealed at 500 °C

3.1.a. Structural properties and composition

The XRD patterns of 120 nm VO_2 thin film grown on silicon substrate by balanced HiPIMS and annealed at 500 °C is shown in *Fig. 3a*. The (011), (200), (020) and (021) Bragg peaks in the pattern confirmed that the as-deposited VO_2 thin film is polycrystalline VO_2(M) (JCPDS 44-0252). Clearly, the (011) is the main diffraction peak, resulting probably from preferential sputtering caused by the energetic bombardment during the HiPIMS process [21]. *Fig. 3b* displays the RBS spectrum of the VO_2 film with the corresponding simulation. The high energy ions scattered by collisions involve coulombic repulsion between the positively charged nuclei of the incident He ions and the target particles. The intensity of the RBS signal

depends on the scattering cross-section, which is directly proportional to the square of the atomic number of the element. V with higher atomic number shows clear isolated peak. Si, being the substrate, results in signal below channel number 1320. Oxygen signal on the Si signal is detected as a peak around channel number 900. The distinct V signal combined with the O signal allows the determination of the stoichiometry of the film from simulated spectrum. The number of incident He ions which are backscattered is also proportional to the number-density of the target atoms along the penetration path. Knowing the thickness, the density of the film can be determined using the following formula:

$$\rho = \frac{A(Vanadium) \times M(Vanadium) + A(Oxygen) \times M(Oxygen)}{N_A \times e}$$

where ρ is the density of the film in $g.cm^{-3}$, A is amounts of element in $atoms.cm^{-2}$, M is molar mass of element in $g.mol^{-1}$, N_A is the Avogadro constant in $atoms.mol^{-1}$ and e is the thickness of the film in cm.

The composition was estimated at $VO_{1.99\pm0.02}$ and the density at 4.37 $g.cm^{-3}$, which is very close (i.e. ≈ 95 %) to the theoretical density of VO_2 = 4.57 $g.cm^{-3}$.

3.1.b. Thermochromic properties

In order to reveal the switching behavior of the VO_2 thin film deposited by balanced HiPIMS and annealed at 500 °C, several measurements as a function of temperature were performed.

Fig. 4a shows the temperature dependence of the resistivity of the film deposited on silicon substrate during a heating/cooling cycle between 20 °C and 100 °C. The oxide transits from semi-conductive state to metallic state during the heating process. Consequently, the resistance of the VO_2 film decreases over three orders of magnitude across the phase transition. Nevertheless, the reversible transformation during the cooling does not occur at the same temperature, which induced a hysteresis loop. The nature of the hysteresis curves

depends very strongly on the competing effects of crystallinity and grain size [22]. The deviation in crystal perfection is known to change the abruptness of the transition as well as the temperature spread of the hysteresis loop [23]. Bulk single crystals tend to show negligible hysteresis (< 2 °C), while thin films usually present a 5 to 15 °C window. The hysteresis width of the phase transition was determined by calculating and plotting dρ/dT against T (*Fig. 4b*). A hysteresis width of 7.5 °C is found and the average transition temperature Tc = [Tc(H) + Tc(C)]/2 is 67.3, which is very close to the Tc of the bulk VO_2 ~ 68 °C.

Phase transition of the prepared VO_2 thin film on silicon substrate was also analysed by optical characterization. *Fig. 5a* illustrates the transmittance measurements carried out during the heating from 20 °C to 90 °C at normal incidence in the spectral domain ranging from 2.0 µm to 25 µm. Silicon substrate contribution was removed by dividing the transmittance sample signals by the nude silicon transmittance. Uncertainty could be estimated at ± 2 % for the measured spectra and ± 1 °C for the temperature. As expected, the optical transmittance exhibits strong change as the temperature increases, indicating a pronounced thermochromic behaviour. The low temperature spectrum exhibits distinct phonon vibration peaks at 16.1 µm and 19.9 µm, attributed to the O-V-O octahedral bending modes in the semi-conductive state. However, these values are slightly different from those obtained for a VO_2 thin film elaborated with a conventional magnetron sputtering suggesting a distortion effect caused by the energetic HiPIMS deposition process. Indeed, as earlier reported [24], the bending modes appeared at 16.6 µm and 19.2 µm for VO_2 thin film deposited by PDCMS (pulsed direct current magnetron sputtering).

With increasing temperature, the octahedral bending modes progressively disappear, due to the transition from the semi-conductive state to the metallic state of VO_2. Simultaneously, a drop in transmittance is observed, due to an increase in reflectivity. A very efficient change in transmittance is observed in the IR spectral region.

To fully investigate the thermochromic behaviour of VO_2 from optical transmittance, measurements were also performed upon the cooling step to generate a complete cycle. *Fig. 5b* shows the thermal hysteresis loop of the intrinsic transmittance-temperature plot at a fixed wavelength of 10 µm. The film exhibits a very nice transmittance switch of nearly 90 % at this wavelength. The switching temperature values during heating [Tc(H)] and cooling [Tc(C)] were deducted from full width at half maximum (FWHM). The hysteresis width is about 6.5 °C, which is close to the value obtained from resistivity measurements. It is interesting to note that the hysteresis width is twice less than that recorded for VO_2 thin films deposited with a conventional PDCMS supply [24]. The abrupt and effective infrared transition observed in the current study can be correlated to the film high crystallinity and density induced by HiPIMS process.

However, the average transition temperature of 64.3 °C remains a bit lower than the Tc obtained by resistivity measurements. This slight difference can be explained by the fact that the electrical behaviour depends strongly on the continuity established between the grains forming the film (i.e. grain boundaries contribution), whereas the interaction of the light is an averaged-out effect on the wavelength scale. In the latter case, even if continuity does not exist between the grains, light is affected by the phase transformation these grains undergo.

In order to determine refractive index and extinction coefficient in both semi-conductive and metallic states of VO_2, fitting from transmittance measurements was carried out at 25 °C and 90 °C using WVASE 32 software. An optical model that describes the sample structure is used to generate predicted data. The mean-squared error (MSE) represents a sum of the squares of the differences between the measured and calculated points. The goal is to compare generated and experimental data and to adjust the model parameters to minimize the MSE value. First, an accurate fitting of the silicon wafer has to be determined.

The optical simulation of the silicon wafer was constructed with a classical Lorentz oscillator model. The transmittance simulated from the model matches the experimental data (*Fig. 6a*). The semi-conductive phase of VO_2 layer was then parametrized using a series of Lorentzian oscillators. An additional Drude term was added to take into account the contribution of the free carriers in the metallic phase. *Fig. 6b* shows the simulated transmittance of VO_2 on silicon substrate at 25 °C and 90 °C. A very nice correspondence between the experimental and fitted curves is observed allowing to validate the optical model used. The optical constants of VO_2 were then deduced from the curve fitting parameters. The evolution of the refractive index (n) and the extinction coefficient (k) of VO_2 in the wavelength range 2–25 µm is shown in *Fig. 6c* and *Fig. 6d* respectively. The refractive index at 25 °C oscillates around 3, while the extinction coefficient is very small (< 0.1) for 2–12 µm. However, an increase in k reaching a maximum value of 3 is observed at about 16 µm and 20 µm. This increase is related to the phonon vibration existing in the semi-conductive state of VO_2. At 90 °C, the values of n and k are totally different compared with those obtained at low temperature. The refractive index n increases rapidly from about 2 to 9 with increasing wavelength from 2 to 9 µm. Then, it decreases to 8 at about 10.5 µm. Further increase in wavelength leads to an increase in n. The extinction coefficient k has a similar behaviour to that of n, overall increasing from 4 to 11 between 2 to 25 µm. The current (n,k) indices are in good agreement with the indices reported for VO_2 films deposited by conventional radio frequency magnetron sputtering [12, 25].

In order to further evaluate the IR properties of VO_2, the thermal radiative flux emitted by a 120 nm VO_2 thin film deposited on glass substrate by balanced HiPIMS was studied by means of an IR camera and compared with a nude glass substrate. During the measurement, the VO_2/glass sample was placed right next to a nude glass on a temperature controlled plate. In agreement with the Stefan-Boltzmann relationship, the radiance power (M) emitted from

the surface of an object can be expressed as $M = \varepsilon\sigma T^4$, where σ is the Stefan-Boltzmann constant and T is the absolute temperature. The camera detects the radiation emitted by the surface of an object and converts the thermal signals into an electronic image. With the knowledge of the body emissivity, its real temperature (T_r) can be determined. In this work, the default emissivity in the LWIR camera was set to 0.90, corresponding to the emissivity of the glass substrate. The apparent temperature (T_{app}) represents the temperature at which the radiance of a gray body with emissivity of 0.90 is equal to that of the sample at Tr. We can thus obtain $T_{app} = (\varepsilon/0.90)^{1/4} \times T_r$, meaning that the measured object temperature T_{app} can be underestimated if the actual emissivity is lower than 0.90. In the case of the glass substrate, $T_r = T_{app}$.

Fig. 7 shows the thermal images recorded by the IR camera at 45 °C and 80 °C across a line allowing to measure simultaneously the apparent temperatures (T_{app}) of both glass substrate and VO_2/glass samples. The two samples have the same apparent temperature at T_r = 45 °C (*Fig. 7a*). At such a temperature, VO_2 is completely transparent in the 7.5-13 µm range, as shown in *Fig. 5* (corresponding to the LWIR window of the camera), so the high emissivity of the glass substrate determines the emissivity of the VO_2/glass sample. Thus, the thermal signal emitted by the VO_2/glass sample is the same as the nude glass substrate. Consequently, both samples exhibit the same apparent temperature. At T_r = 80 °C (*Fig. 7b*), the VO_2 thin film is IR reflective; most of the thermal fluxes emitted by the substrate are reflected by the VO_2 metallic state. Thus the VO_2/glass shows a low emissivity with an apparent temperature of only 40 °C, i.e. the sample appears even cooler than at T_r = 45 °C. So, the VO_2/glass sample exhibits chameleon-like behaviour in the LWIR region, that such an object is difficult to be detected using an IR camera, irrespective of its real temperature and can be used for adaptive camouflage applications [6, 26].

To conclude on these first results, a pure polycrystalline VO_2(M) thin film was successfully prepared by balanced HiPIMS. The film annealed at 500 °C revealed excellent IR thermochromic properties with a transition temperature close to the Tc in bulk VO_2. Thereafter, the objective was to achieve VO_2 thin film with such a nice thermochromic behaviour, but annealed at lower temperature aiming at enlarging the nature of substrates to be used.

3.2. Study of VO_2 thin films prepared by balanced HiPIMS and annealed at lower temperature

The effect of the annealing temperature on thermochromic properties of VO_2 thin films deposited by balanced HiPIMS is studied in this section.

XRD patterns of 120 nm VO_2 thin films grown on silicon substrate and annealed at 400 °C and 300 °C are shown in *Fig. 8a*. XRD pattern of the VO_2 film annealed at 500 °C and investigated in the first section is also displayed for comparison. It can be noticed that monoclinic VO_2 phase is obtained for the film annealed at 400 °C, however showing lower crystallinity (i.e. decrease in XRD peak intensity). For the film annealed at 300 °C, an additional peak at around 2θ = 25 ° appears. This peak belongs to the (110) peak of non thermochromic metastable VO_2(B) phase [27], which is usually obtained for temperature lower than 400 °C [12]. The energy provided by the thermal treatment is not high enough to fully crystallize the film in thermochromic VO_2(M) phase. The average crystallite size D (nm) in each film was calculated from Debye-Scherrer formula defined as follows: $D = \frac{0.9 \times \lambda}{\beta \times \cos\theta}$

where λ, β and θ are the incident X-ray wavelength, the half width of the maximum diffraction peak and the angle between the incident beam and crystal plane respectively. *Table 1* presents values of D obtained from (011) VO_2(M) peak. All films possess nano-crystalline structure. A strong decrease of crystallite size with the decrease of annealing temperature is

observed. *Fig. 8b* shows the thermal hysteresis curve of the intrinsic transmittance-temperature plot at a fixed wavelength of 10 µm for the films annealed at 400 °C and 500 °C. The optical performance of each film is also gathered in *Table 1*. A clear degradation in thermochromic properties is detected for the film annealed at 400 °C. Indeed, the infrared transmittance modulation ΔTr (%) determined from the difference between the lowest and the highest temperature states decreases from 89% to 66%. The average transition temperature also decreases from around 64 °C to 54 °C. This thermochromic behaviour change results directly from a lower crystallinity of the film. Other studies proved that polycrystalline VO_2 thin films with a smaller crystallite size possessed lower phase transition temperature [28, 29, 30]. Measurements were also performed for the 300 °C VO_2 thin film, but none transmittance switch was observed, certainly because of very bad crystallinity of VO_2(M) phase and existence of the VO_2(B) phase.

Annealing temperature (°C)	*D ± 0.5 (nm)*	*ΔTc (°C)*	*Tc (°C)*	*ΔTr (%)*
500	22.1	6.5	64.3	89.1
400	11.9	8	54.0	66.4
300	7.4	/	/	/

Table 1. *Crystallite size calculated from Debye-Scherrer formula and thermochromic properties deduced from transmittance hysteresis loops for the VO_2 thin films deposited by balanced HiPIMS (D is the average crystallite size, ΔTc the hysteresis width, Tc the average transition temperature and ΔTr the transmittance modulation).*

3.3. Study of VO_2 thin films prepared by unbalanced HiPIMS

In this section, VO_2 thin films were deposited by unbalanced HiPIMS. XRD patterns of 120 nm VO_2 thin films grown on silicon substrate by unbalanced HiPIMS and annealed at 500 °C, 400 °C and 300 °C are shown in *Fig. 9a*. It can be seen that the dominant crystalline phase in all three films is the desired thermochromic VO_2(M) phase even for the sample annealed at only 300 °C. The high energy delivered into the growing films, thanks to the

unbalanced magnetron configuration, probably allows to start crystallisation mechanism during the deposition process, leading to the possible formation of a pure VO_2(M) phase by the 300 °C post-annealing treatment. The thermal transmittance hysteresis curves plot at a fixed wavelength of 10 µm are shown in *Fig. 9b*. The crystallite size of the films, calculated from Debye-Scherrer formula, and the optical performance of the films are gathered in *Table 2*. Crystallite size slightly decreases from 21.7 nm to 18.3 nm with the decrease of annealing temperature from 500 °C to 300 °C. Thus, the decrease of annealing temperature does not really affect the crystallite size of VO_2, unlike the films deposited by balanced HiPIMS, for which the crystallite size strongly decreases when the annealing temperature is reduced to 300 °C (cf. *Table 1*). This demonstrates once again benefits of using unbalanced HiPIMS to elaborate highly crystallizedVO_2 thin films at lower annealing temperature.

The films annealed at 500 °C and 400 °C exhibit a similar thermochromic behavior with a very nice optical modulation reaching nearly 90 %. On the contrary to the films deposited by balanced HiPIMS, the decrease of annealing temperature from 500 °C to 400 °C preserved both structural properties and optical performance. The film annealed at 300 °C transits at a lower temperature than the two other ones (59 °C compared to around 63 °C). All the films have the same high transmittance value at room temperature, whilst at 90 °C the film annealed at 300 °C exhibits a poorer metallic state (i.e. higher transmittance value). Consequently, an optical modulation of 71.5 % is obtained for the film annealed at 300 °C, which is a bit lower than that of the two other films. A lower crystallinity and a lower film density due to the decrease of the annealing temperature could explain such results.

Annealing temperature (°C)	*D ± 0.5 (nm)*	*ΔTc (°C)*	*Tc (°C)*	*ΔTr (%)*
500	21.7	8.0	63.5	89.1
400	19.6	9.0	63.0	88.3
300	18.3	11.0	59.0	71.5

Table 2. *Crystallite size calculated from Debye-Scherrer formula and thermochromic properties deduced from transmittance hysteresis loops for the VO_2 thin films deposited by*

unbalanced HiPIMS (D is the average crystallite size, ΔTc the hysteresis width, Tc *the average transition temperature and ΔTr the transmittance modulation).*

The resistivity-temperature curve of the VO_2 film deposited by unbalanced HiPIMS and annealed at 300 °C is displayed in *Fig. 10a*. A drop in resistivity by almost two orders of magnitude is observed at around 60 °C, confirming a thermochromic behaviour of the VO_2 film. A hysteresis width of 14 °C is found from dρ/dT against T curve (*Fig. 10b*).

4. Conclusion

High quality stoichiometric polycrystalline thermochromic VO_2 thin films were successfully prepared using both balanced and unbalanced HiPIMS process. Different annealing temperatures from 300 to 500 °C allow the fabrication of functional thermochromic VO_2 thin films. The optical properties of the as-prepared films were fully investigated by mid-infrared transmittance measurements. Excellent thermochromic properties were obtained with the two magnetron configurations when the annealing temperature reaches 500 °C. However, a decrease in annealing temperature was accompanied by a pronounced degradation of the optical and structural performances for the films deposited by balanced HiPIMS. On the contrary, VO_2 films deposited by unbalanced HiPIMS showed very nice thermochromic behaviour even when the annealing temperature was reduced to only 300 °C. The magnetic field induced by the unbalanced magnetron provides extra energy to the sputtered species, allowing a better migration of adatoms on the substrate surface. Thus, a lower annealing temperature is then required to crystallize the films. All the films were deposited at room temperature without bias substrate or crystalline interlayer, which are usually used to assist crystallization of thermochromic VO_2. Due to the possibility of tuning the ion flux and plasma density, as well as the ion bombardment characteristics at the growing film surface,

unbalanced HiPIMS process appears very promising and industry-friendly for the fabrication of polycrystalline thermochromic coatings at lower temperature.

CRediT author statement

Jean-Louis Victor: Conceptualization, Deposition, Characterization, Original draft preparation. **Corinne Marcel:** Supervision, Revision. **Laurent Sauques:** Supervision. **Nicolas Penin:** Resistivity Characterization, Revision. **Aline Rougier:** Supervision, Writing - Revision.

Acknowledgements

The authors would like to thank Mathieu Taillebosc and Dr. Frédéric Chapelet from Optronic Department of DGA Toulouse Center for their help in IR camera utilization. The authors also want to thank Frédéric Amiard and Dr. Alain Gibaud from IMMM Department of Le Man University for their help in transmittance measurements.

Declaration of competing interest

The authors declare that they have no known competing financial interests or personal relationships that could have appeared to influence the work reported in this paper.

References

[1] H. Ling, J. Wu, F. Su, Y. Tian and Y. Liu, "Automatic light-adjusting electrochromic device powered by perovskite solar cell," *Nature Communications* , vol. 12, no. 1010, pp. 1-8, 2021.

[2] A. Dokouzis, F. Bella, K. Theodosiou, C. Gerbaldi and G. Leftheriotis, "Photoelectrochromic devices with cobalt redox electrolytes," *Materials Today Energy,* vol. 15, no. 100365, pp. 1-8, 2020.

[3] A. Carella, R. Centore, F. Borbone, M. Toscanesi, M. Trifuoggi, F. Bella, C. Gerbaldi, S. Galliano, E. Schiavo, A. Massaro, A. Munoz-García and M. Pavone, "Tuning optical and electronic properties in novel carbazole photosensitizers for p-type dye-sensitized solar cells," *Electrochimica Acta*, vol. 292, pp. 805-816, 2018.

[4] A. Zylbersztejn and N. F. Mott, "Metal-insulator transition in vanadium dioxide," *Phys. Rev. B*, vol. 11, pp. 4383-4395, 1975.

[5] W. J. M. Kort-Kamp, S. Kramadhati, A. K. Azad, M. T. Reiten and D. A. R. Dalvit, "Passive Radiative “Thermostat” Enabled by Phase-Change Photonic Nanostructures," *ACS Photonics,* vol. 5, pp. 4554-4560, 2018.

[6] L. Xiao, H. Ma, J. Liu, W. Zhao, Y. Jia, Q. Zhao, K. Liu, Y. Wu, Y. Wei, S. Fan and K. Jiang, "Fast Adaptive Thermal Camouflage Based on Flexible VO_2/Graphene/CNT Thin Films," *Nano Letters,* vol. 15, pp. 8365-8370, 2015.

[7] Y. Cui, Y. Ke, C. Liu, Z. Chen, N. Wang, L. Zhang, Y. Zhou, S. Wang, Y. Gao and Y. Long, "Thermochromic VO_2 for Energy-Efficient Smart Windows," *Joule,* vol. 2, pp. 1707-1746, 2018.

[8] B. Rajeswaran and A. M. Umarji, "Defect engineering of VO_2 thin films synthesized by Chemical Vapor Deposition," *Materials Chemistry and Physics,* vol. 245, pp. 1-8, 2020.

[9] D. Liu, H. Cheng, X. Xing, C. Zhang and W. Zheng, "Thermochromic properties of W-doped VO_2 thin films deposited by aqueous sol-gel method for adaptive infrared stealth application," *Infrared Physics & Technology,* vol. 77, pp. 339-343, 2016.

[10] R. McGee, A. Goswami, B. Khorshidi, K. McGuire, K. Schofield and T. Thundat, "Effect of process parameters on phase stability and metal-insulator transition of vanadium dioxide (VO_2) thin films by pulsed laser deposition," *Acta Materialia,* vol. 137, pp. 12-21, 2017.

[11] Y. Y. Luo, S. S. Pan, S. C. Xu, L. Zhong, H. Wang and G. H. Li, "Influence of sputtering power on the phase transition performance of VO_2 thin films grown by magnetron sputtering," *Journal of Alloys and Compounds,* vol. 664, pp. 626-231, 2016.

[12] F. Guinneton, L. Sauques, J. Valmalette, F. Cros and J. Gavarri, "Optimized infrared switching properties in thermochromic vanadium dioxide thin films: role of deposition process and microstructure," *Thin Solid Films,* vol. 446, pp. 287-295, 2003.

[13] P. C. Juan, K. C. Lin, C. L. Lin, C. A. Tsai and Y. C. Chen, "Low thermal budget annealing for thermochromic VO_2 thin films prepared by high power impulse magnetron sputtering," *Thin Solid Films* , vol. 687, pp. 1-8, 2019.

[14] T. D. Vu, S. Liu, X. Zeng, C. Li and Y. Long, "High-power impulse magnetron sputtering deposition of high crystallinity vanadium dioxide for thermochromic smart windows applications," *Ceramics International,* vol. 46, pp. 8145-8153, 2020.

[15] S. Dou, W. Zhang, F. Ren, J. Gu, H. Wei, X. Chen, G. Xu, X. Yan, Y. Zhan, J. Zhao and Y. Li, "The infrared optical performance of VO_2 film prepared by HiPIMS," *Materials Chemistry and Physics,* vol. 259, pp. 1-8, 2021.

[16] A. Ferrec, J. Keraudy, S. Jacq, F. Schuster, P. Y. Jouan and M. A. Djouadi, "Correlation between mass-spectrometer measurements and thin film characteristics using dcMS and HiPIMS discharges," *Surface & Coatings Technology,* vol. 250, pp. 52-56, 2014.

[17] J. P. Fortier, B. Baloukas, O. Zabeida, J. E. Klemberg-Sapieha and L. Martinu, "Thermochromic VO_2 thin films deposited by HiPIMS," *Solar Energy Materials & Solar Cells,* vol. 125, pp. 291-296, 2014.

[18] A. Aijaz, Y. X. Ji, J. Montero, G. A. Niklasson and C. G. Granqvist, "Low-temperature synthesis of thermochromic vanadium dioxide thin films by reactive high power impulse magnetron sputtering," *Solar Energy Materials & Solar Cells,* vol. 149, pp. 137-144, 2016.

[19] J. Houska, D. K. J. Vlcek and R. Cerstvy, "Properties of thermochromic VO_2 films prepared by HiPIMS onto unbiased amorphous glass substrates at a low temperature of 300 °C," *Thin Solid Films,* vol. 660, pp. 463-470, 2018.

[20] G. Shanker, P. Prathap, K. M. K. Srivatsa and P. Singh, "Effect of balanced and unbalanced magnetron sputtering processes on the properties of SnO_2 thin films," *Current Applied Physics,* vol. 19, pp. 697-703, 2019.

[21] K. Sarakinos, J. Alami and S. Konstantinidis, "High power pulsed magnetron sputtering:

a review on scientific and engineering state of the art," *Surface & Coatings Technology*, pp. 1661 - 1684, 2004.

[22] C. Zhang, C. Koughia, O. Güneş, J. Luo, N. Hossain, Y. Li, X. Cui, S.-J. Wen, R. Wong, Q. Yang and S. Kasap, "Synthesis, structure and optical properties of high-quality VO_2 thin films grown on silicon, quartz and sapphire substrates by high temperature magnetron sputtering: Properties through the transition temperature," *Journal of Alloys and Compounds*, vol. 848, pp. 1-13, 2020.

[23] P. Ashrit, "Thermochromic Thin Films and Devices," *Transition Metal Oxide Thin Film based Chromogenics and Devices*, pp. 153-246, 2017.

[24] J. L. Victor, C. Marcel, L. Sauques, C. Labrugere, F. Amiard, A. Gibaud and A. Rougier, "From multilayers to $V_{1-x}W_xO_{2\pm d}$ films elaborated by magnetron sputtering for decreasing thermochromic transition temperature," *Journal of Alloys and Compounds*, pp. 1-7, 2020.

[25] M. Benkahoul, M. Chaker, J. Margot, E. Haddad, R. Kruzelecky, B. Wong, W. Jamroz and P. Poinas, "Thermochromic VO_2 film deposited on Al with tunable thermal emissivity for space applications," *Solar Energy Materials & Solar Cells*, vol. 95, pp. 3504-3508, 2011.

[26] D. Liu, H. Ji, R. Peng, H. Cheng and C. Zhang, "Infrared chameleon-like behavior from VO_2(M) thin films prepared by transformation of metastable VO_2(B) for adaptive camouflage in both thermal atmospheric windows," *Solar Energy Materials and Solar Cells*, vol. 185, pp. 210-217, 2018.

[27] J. C. Valmalette and J. R. Gavarri, "High efficiency thermochromic VO_2(R) resulting from the irreversible transformation of VO_2(B)," *Materials Science and Engineering* , vol. B54 , p. 68 – 173, 1998.

[28] J. Jian, W. Zhang, C. Jacob, A. Chen, H. Wang, J. Huang and H. Wang, "Roles of grain boundaries on the semiconductor to metal phase transition of VO_2," *Appl. Phys. Lett.*, vol. 107, pp. 1-5, 2015.

[29] M. J. Miller and J. Wang, "Influence of grain size on transition temperature of thermochromic VO_2," *J. Appl. Phys.*, vol. 117, pp. 1-6, 2015.

[30] T. Lin, L. Wang, X. Wang, Y. Zhang and Y. Yu, "Influence of bias voltage on microstructure and phase transition properties of VO_2 thin film synthesized by HiPIMS," *Surface & Coatings Technology*, vol. 305, pp. 110-115, 2016.

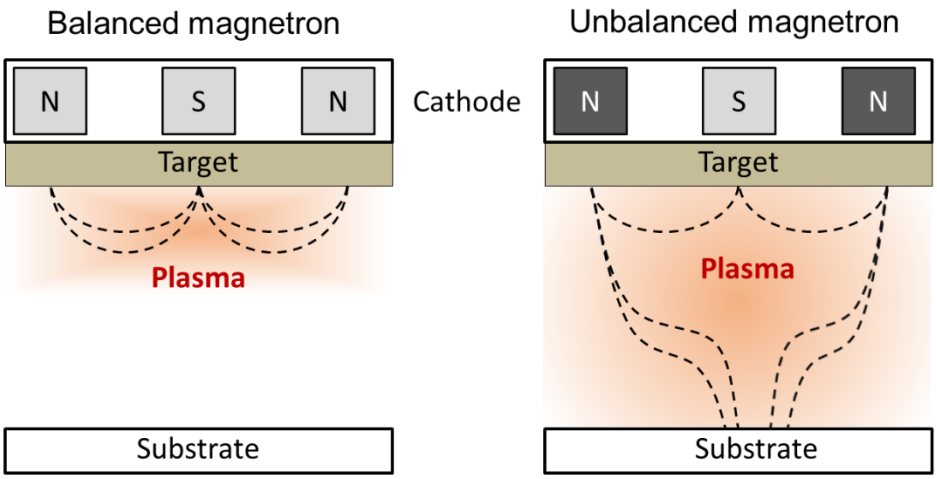

Fig. 1. Balanced and unbalanced magnetron sputtering configurations.

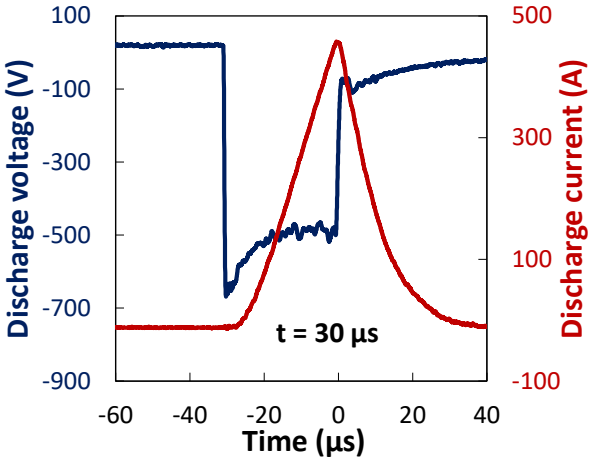

Fig. 2. Discharge current and voltage vs. time during the HiPIMS process.

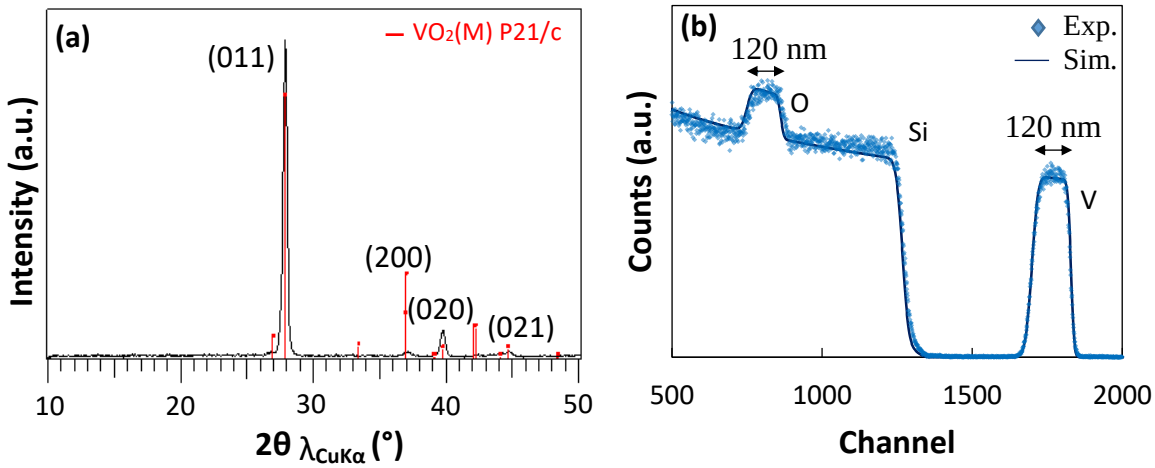

Fig. 3. X-ray diffraction pattern from θ-2θ scans (a) and RBS spectrum (b) of 120 nm VO2 thin film deposited on silicon substrate by balanced HiPIMS. (For interpretation of the references to colour in this figure legend, the reader is referred to the Web version of this article.)

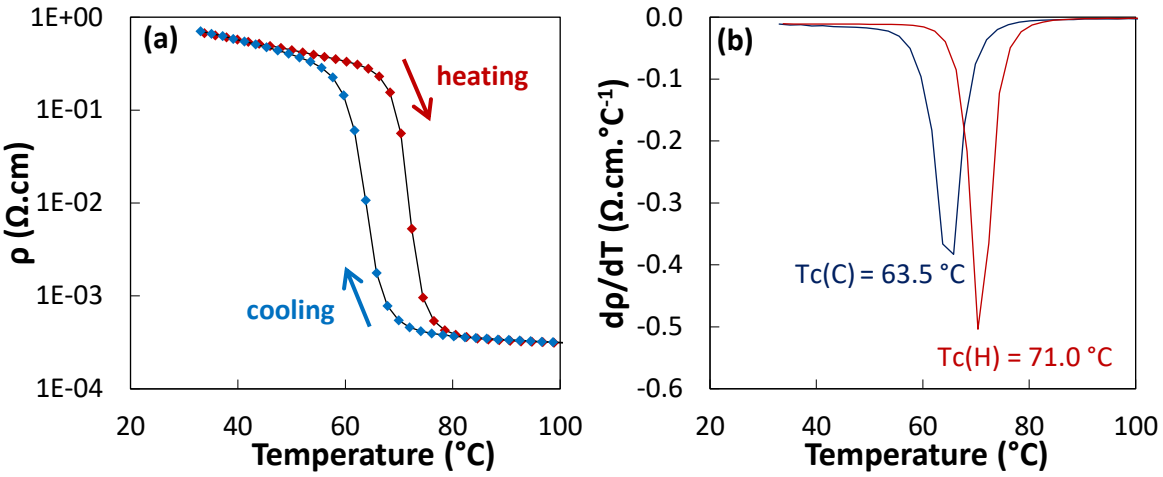

Fig. 4. Temperature dependence of the electrical resistivity for a 120 nm VO2 thin film deposited on silicon substrate by balanced HiPIMS and annealed at 500 °C (a) and first derivative of the resistivity as a function of temperature (b). (For interpretation of the references to colour in this figure legend, the reader is referred to the Web version of this article.)

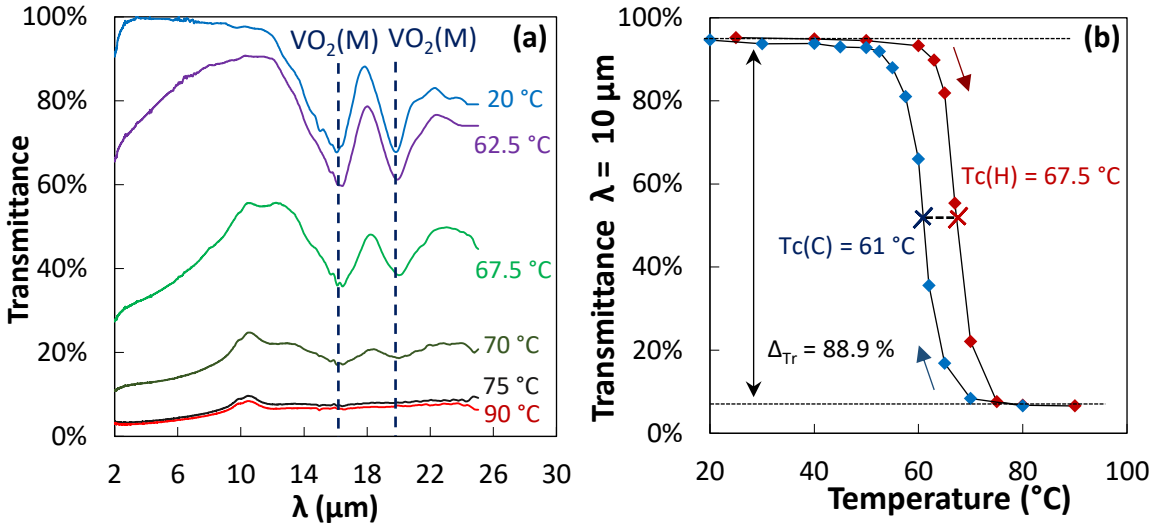

Fig. 5. Variable temperature infrared transmittance spectra of 120 nm VO2 thin film deposited by balanced HiPIMS during the heating phase (a) and hysteresis loop from transmittance values at 10 µm (b).

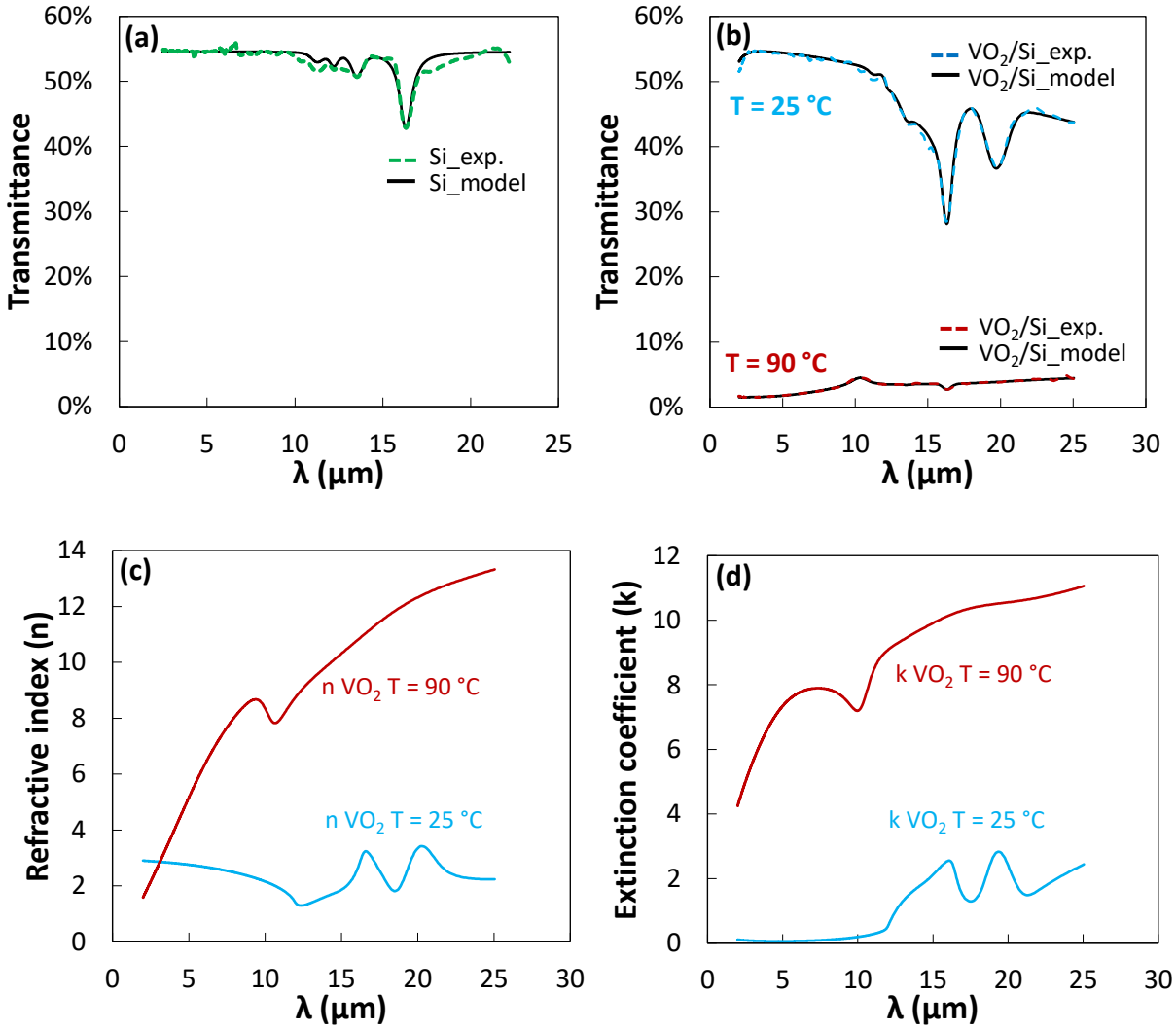

Fig. 6. Experimental and simulated transmittance for the silicon wafer (a) experimental and simulated transmittance of VO2 thin film on silicon substrate plotted a 25 °C and 90 °C, (b) refractive index (c) and extinction coefficient (d) of VO2 deduced from the curve fitting parameters. (For interpretation of the references to colour in this figure legend, the reader is referred to the Web version of this article.)

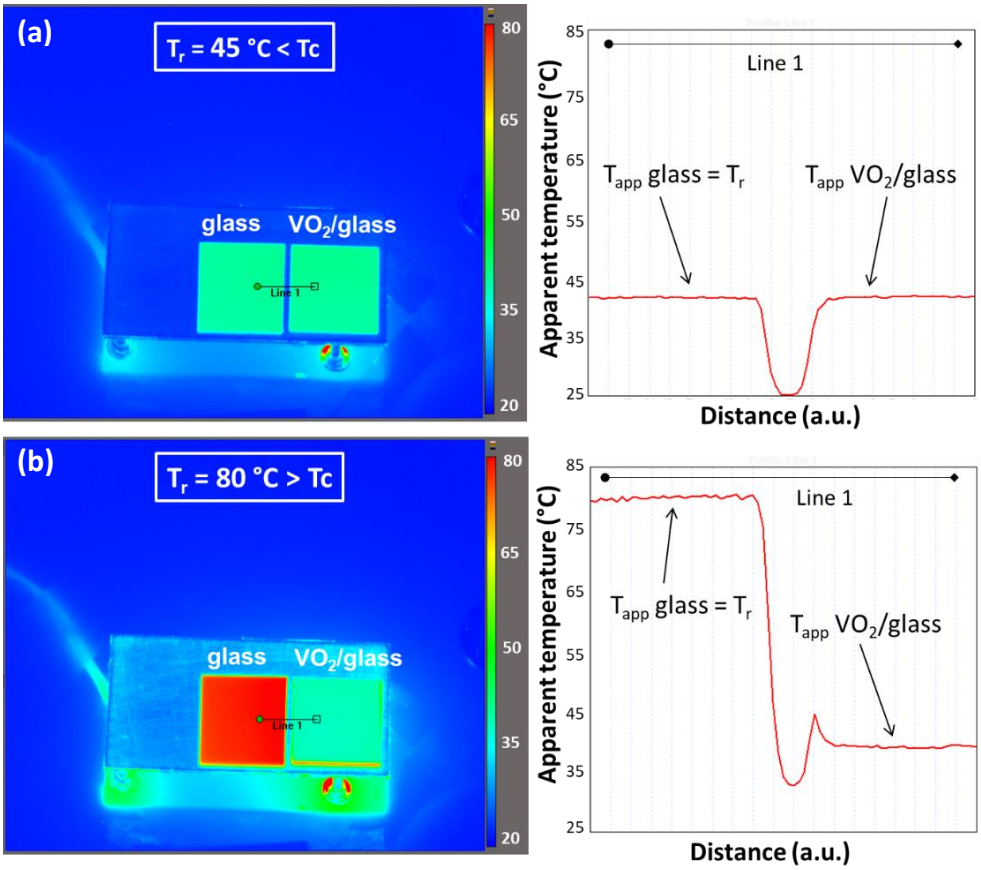

Fig. 7. Thermal images recorded by the IR camera at 45 °C (a) and 80 °C (b) and the measured apparent temperature for a nude glass substrate and VO2/glass sample.

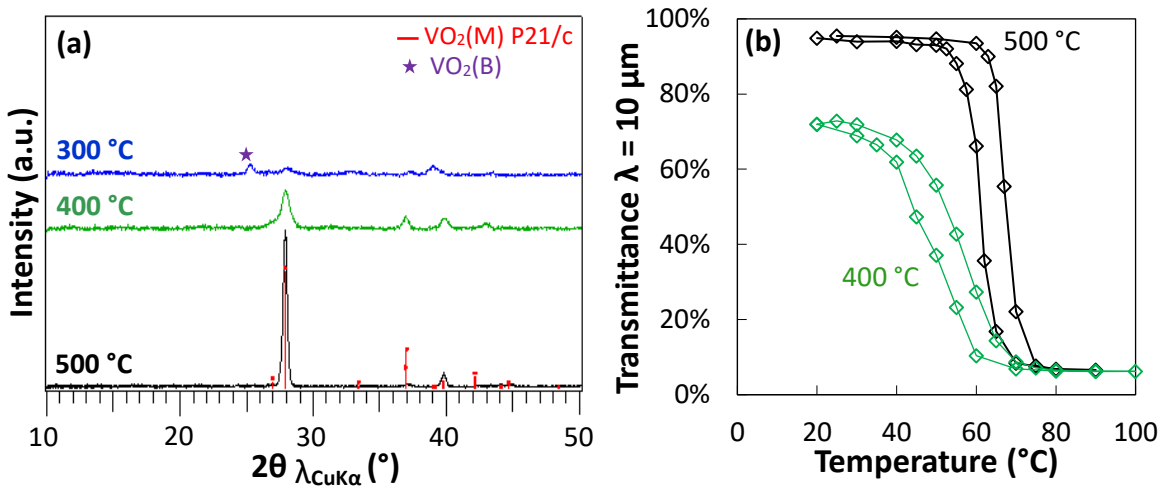

Fig. 8. X-ray diffraction patterns from θ-2θ scans of 120 nm VO2 thin films deposited on silicon substrate by the balanced HiPIMS and annealed at 500 °C, 400 C, 300 C (a) and hysteresis curve from transmittance values at 10 µm (b) (data recorded at 300 C are not displayed because none optical switch was observed for this sample). (For interpretation of the references to colour in this figure legend, the reader is referred to the Web version of this article.)

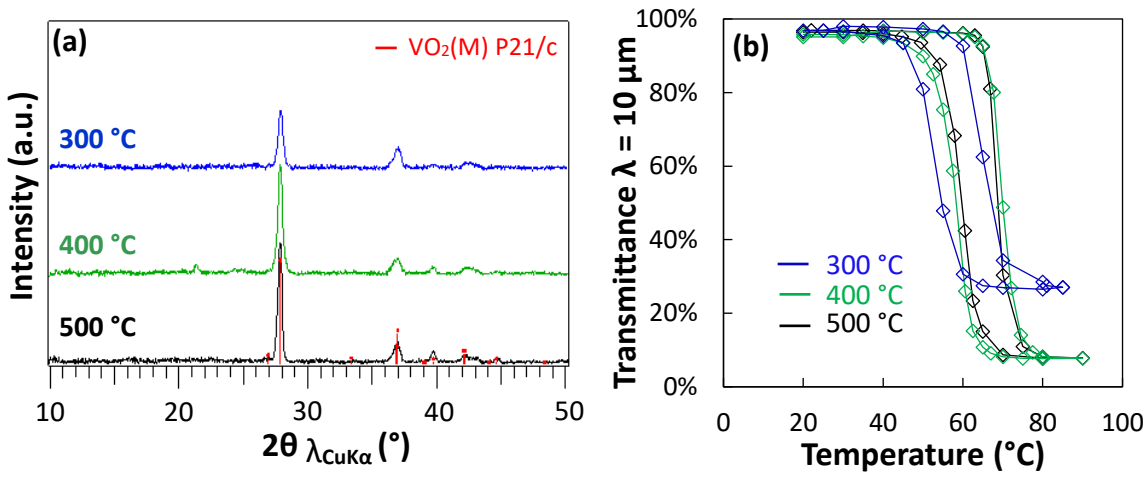

Fig. 9. X-ray diffraction pattern from θ-2θ scans of 120 nm VO2 thin films deposited on silicon substrate by the unbalanced HiPIMS and annealed at 500 °C, 400 °C, 300 °C (a) and hysteresis curve from transmittance values at 10 µm (b). (For interpretation of the references to colour in this figure legend, the reader is referred to the Web version of this article.)

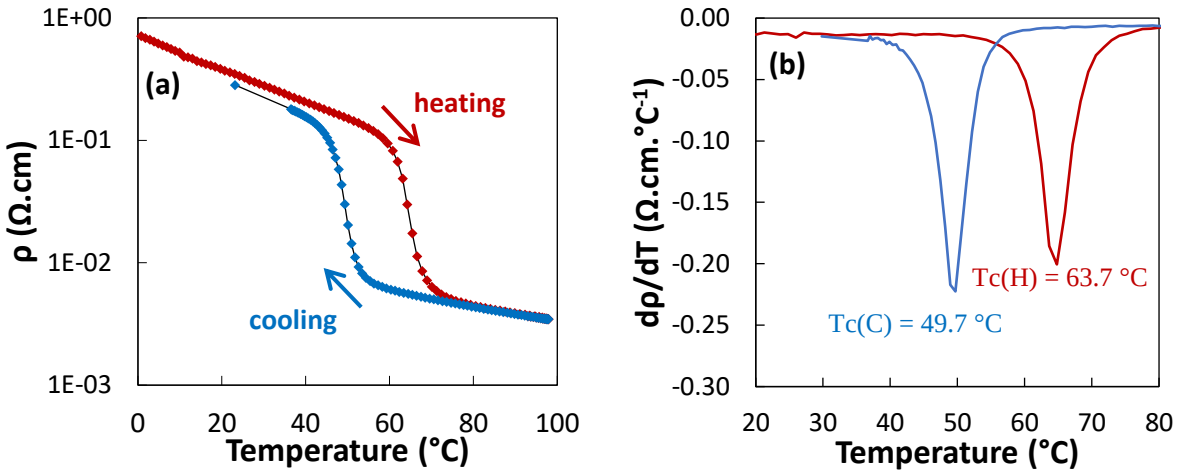

Fig. 10. Temperature dependence of the electrical resistivity for the VO2 film annealed at 300 °C (a) and first derivative of the resistivity as a function of temperature (b).